Nuclear Instruments and Methods 217 (1983) 405–417
North-Holland Publishing Company

A SEGMENTED PHOTON–HADRON CALORIMETER USING A TWO COLOURED WAVELENGTH SHIFTER OPTICAL READOUT SYSTEM

C. DE MARZO, M. DE PALMA, A. DISTANTE, C. FAVUZZI, R. FERRORELLI, P. LAVOPA, G. MAGGI, M. PERCHIAZZI, F. POSA, A. RANIERI, G. SELVAGGI, P. SPINELLI and F. WALDNER

Dipartimento di Fisica dell'Università di Bari and Istituto Nazionale de Fisica Nucleare, Bari, Italy

J. FENT, P. FREUND, H. FESSLER, R. KALBACH †, A. MANZ, P. POLAKOS, K.P. PRETZL, T. SCHOUTEN, P. SEYBOTH, J. SEYERLEIN and D. VRANIC §

Max-Planck-Insitut für Physik und Astrophysik, München, Germany

Received 2 June 1983

The construction and performance of two segmented scintillator photon and hadron calorimeters (a ring and a downstream calorimeter) are described. They were used in an experiment (NA5) at the CERN SPS to study deep inelastic hadron–hadron collisons. A novel light collection system was developed using acrylic rods doped with two different colour wavelength shifter materials (Yellow 323 and BBQ). This allowed signals from the photon and hadron calorimeter to be transmitted by a common readout rod and rendered a compact and economical construction of the calorimeters.

1. Introduction

The calorimeters described here were used in an experiment (NA5) at the CERN SPS to study deep inelastic hadron–hadron collisions leading to events with large transverse energy E_T [1]. A description of the full NA5 apparatus is given in ref. 2. Two types of calorimeters were employed: a ring calorimeter covering 45° to 135° in the c.m.s. polar angle, θ^*, and 2π in the azimuthal angle, ϕ, with a central hole around the beam axis, and a downstream calorimeter covering the central hole of the ring calorimeter. Both calorimeters consist of two sections: a lead–scintillator sandwich photon section followed by an iron–scintillator sandwich hadronic section.

In order to determine the transverse energy of individual particles the ring calorimeter was segmented into 240 cells each of which covered 9° in θ^* and 15° in ϕ. This fine segmentation of the calorimeter allowed the study of the topology of high-E_T events and in particular the search for jets, which would manifest themselves as energy clusters measured in the calorimeter. A novel light collection system was developed [3] to make the fine segmentation of the calorimeter technically feasible. It will be described in detail in sect. 2.1 of this paper.

The downstream calorimeter was segmented into 4 cells and was used to measure the energy of particles at small angles.

This paper is organised in the following manner: sect. 2 contains the description of the optical readout system, the construction and performance of the ring calorimeter, sect. 3 describes the construction and performance of the downstream calorimeter.

2. Ring calorimeter

As shown in fig. 1 the ring calorimeter is a cylinder with an outer diameter of 3.53 m and a 56 cm central hole. The photon section was made out of 16 layers each consisting of 0.53 cm thick lead which was glued to 1 mm thick aluminum to provide mechanical strength and 1.8 cm thick scintillator. The hadron section contained 20 layers of 5 cm thick iron and 2.5 cm thick scintillator. The calorimeter was divided into 24 azimuthal sectors one of which is shown in fig. 2. Each sector was subdivided radially into 10 individual cells. The total sensitive area of the calorimeter was a circle of 3.0 m diameter excluding a 56 cm central hole around the incident beam axis. Acrylic rods doped with wavelength shifter (w.s.) material were used to read out the scintillator light in each cell. At the downstream end of the calorimeter photomultiplier tubes (PM) were glued to the readout rods (fig. 3).

The calorimeter was mounted on a movable support structure, which allowed the longitudinal distance from

† Deceased.

§ On leave from R. Boskovic Institute, Zagreb, Yugoslavia.

0167-5087/83/0000–0000/$03.00

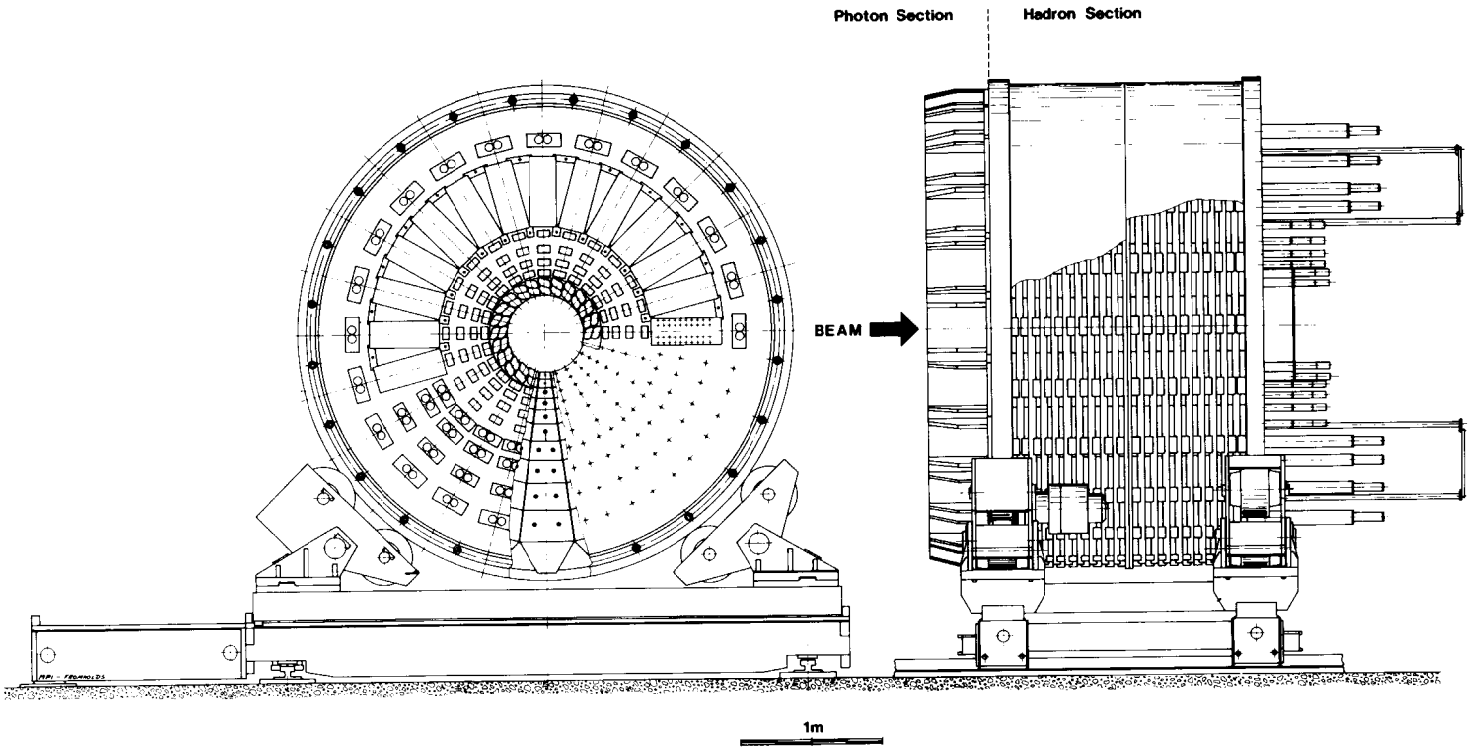

Fig. 1. Front and side view of the ring calorimeter and its support structure. Indicated is one of the 24 sectors of the calorimeter, which is subdivided into 10 individual cells. The photomultipliers are mounted at the downstream end of the calorimeter.

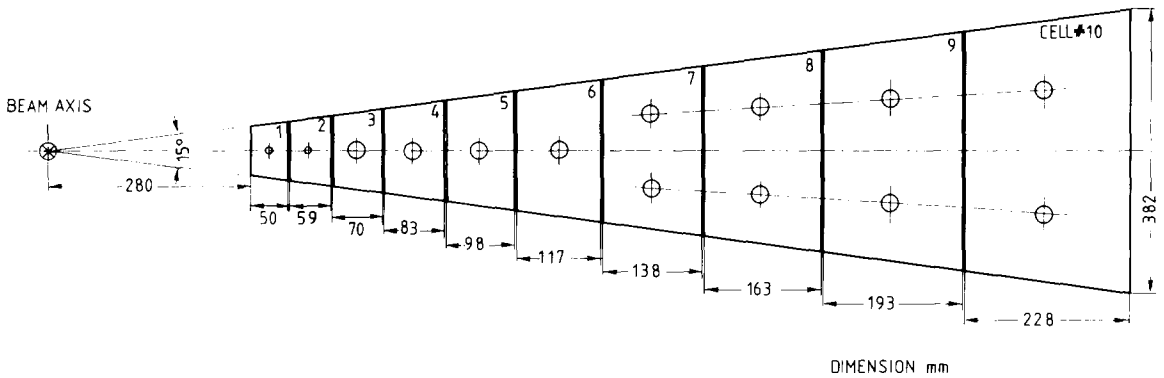

Fig. 2. One of the 24 sectors, which is subdivided into 10 individual cells, is illustrated. Dimensions are in mm.

the experimental target to the calorimeter to be varied. This feature was used when measuring the scaling behaviour of deep inelastic hadron–hadron collisions. This support structure also provided for rotation and transverse motion of the calorimeter. These features were used for calibration purposes, when each calorimeter cell was moved into the incident beam.

2.1. Optical readout system

The optical readout system is based on the use of fluorescent radiation converters described elsewhere [4–6]. As a new application of this principle we used combined w.s. acrylic rods (doped with Yellow 323 * and BBQ ** w.s.) to draw separated signals from the photon and the hadron sections of the calorimeter. Fig. 3 illustrates the principle of the optical readout system. Light from each of a given group of scintillators passes through a small air gap and into a common acrylic rod which is doped with a w.s. material. The isotropically re-emitted fluorescent light is guided along the rod, which passes through holes in the scintillators of one cell as well as through holes in the absorbing material between them. The portion of each rod in the photon calorimeter is doped with the fluorescent converter Yellow 323, which emits yellow light with wavelength of ~ 590 nm. The portion of each rod in the hadron calorimeter is doped with a different converter, namely BBQ which emits green light with wavelength of ~ 490 nm. The two colour components of light resulting from photon and hadron showers respectively are guided in the same rod towards the two PMs. The two colours are separated by two appropriate filters one in front of each PM. For the detection of the yellow light we used a red

* Product of Röhm GmbH, Darmstadt, West Germany.
** Product of Nuclear Enterprises Ltd., Great Britain.

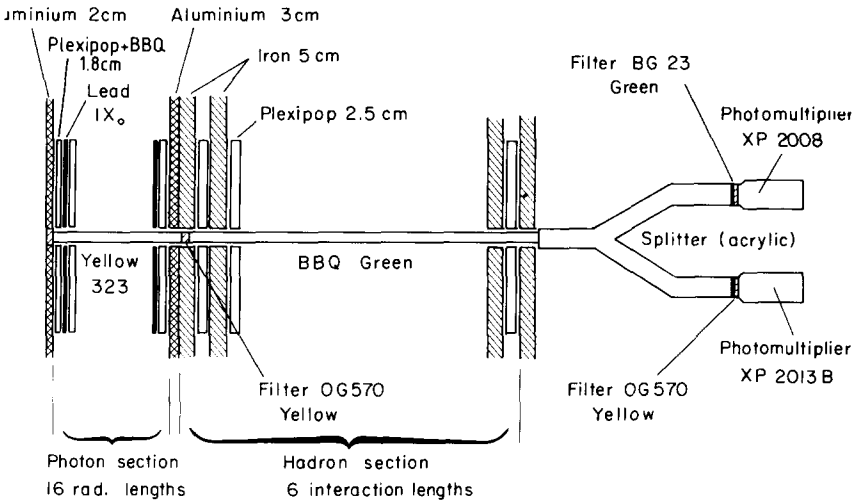

Fig. 3. The principle of the two coloured wavelength shifter optical readout system is illustrated.

Table 1
The scintillator and wavelength shifter rods used in the ring-calorimeter.

Photon section:

	Material	Doped with	Thickness (cm)
Scintillator	Plexipop [a]	3% Naphthalene 1% Butyl PBD 0.03% POPOP 0.004% BBQ	1.8
w.s. rod	Plexi 218 [b]	20 mg/l of Yellow 323	∅ 1 or ∅ 2

Hadron section:

	Material	Doped with	Thickness (cm)
Scintillator	Plexipop [a]	3% Naphthalene 1% Butyl PBD 0.03% POPOP	2.5
w.s. rod	Plexi 218 [b]	75 mg/l of BBQ	∅ 1 or ∅ 2

[a] Manufactured by Polivar, Pomezia, Italy.
[b] Manufactured by Röhm GmbH, Darmstadt, West Germany.

sensitive PM XP 2013 * and a glass filter of the type OG 570 **, which absorbed the green light. For the detection of the green light we used a green sensitive PM XP 2008 * and a glass filter BG 23 **, which absorbed the yellow light. The filters and the PMs were glued with silicone rubber material § onto the light guides. In order to minimize the cross talk between the photon and the hadron section of the calorimeter the two portions of each w.s. rod were glued together with an appropriate optical filter OG 570. This filter absorbs the green light from the hadron calorimeter which otherwise would excite the yellow fluorescent radiator in the rods of the photon section of the calorimeter.

In order to obtain similar light yield from the different size cells one or two readout rods were passed through the cells as indicated by the holes in fig. 2. The diameter of the rods was 1 cm for the cells #1 and #2 and 2 cm for the rest. Each rod or each pair of rods was glued to an optical light splitter made of acryl (PLEXI 218) §§ as shown in fig. 3. In order to avoid Cherenkov light generated in the light splitters near the central hole of the calorimeter we used for cell #1 and #2 reflecting aluminum tubes (air light guides!) instead of acryl. The upstream ends of the readout rods were painted with TiO_2 paint to increase their reflectivity.

The scintillator and w.s. materials used together with their chemical compounds are listed in table 1. Because of the short preparation time for the experiment only materials which were easily available from manufacturers were considered. The optimisation of the light yield in combining Plexipop scintillators with various w.s. rods is described in ref. 3. The quantum efficiency of the Yellow w.s. rods was improved by a factor 3.5 by adding 40 mg/l BBQ to the Plexipop scintillator material in the photon section of the calorimeter. The absorption and emission spectra of the BBQ and Yellow w.s. rods together with the appropriate emission spectra of the scintillator materials are shown in figs. 4a and b for the hadron and photon section of the calorimeter respectively. As can be seen the emission spectrum of the scintillator and the absorption spectrum of the w.s. rods in the photon section are somewhat better matched than in the case of the hadron calorimeter.

The transmission length Λ of each individual w.s. rod was measured. The mean value of Λ and the standard deviation are given in table 2. Those rods with Λ shorter than the mean value minus one standard deviation were rejected.

2.2. Mechanical construction

The principles of the mechanical construction of the ring calorimeter are shown in fig. 5. The photon calorimeter consists of 24 wedge shaped sectors which are bolted to the front iron disk of the hadron calorimeter. The hadron calorimeter consists of 21 iron disks with 5 cm thickness each. The front and back disk of the calorimeter have each a 13.5 cm wide ring which rests on the rollers of the movable support system. Through the iron disks 1.6 cm and 3.0 cm diameter holes were drilled for the passage of the 1 cm and 2 cm diameter w.s. rods respectively. The disks are held together by bolts which are arranged on the perimeter. Spacers were used to keep the disks 3.0 cm apart from each other allowing the insertion of the scintillator material. The scintillator of the hadron calorimeter was

Table 2
The mean value $\bar{\Lambda}$ and the standard deviation σ_Λ of the measured attenuation lengths for the wavelength shifter rods.

w.s. rod doped with	Diameter (cm)	$\bar{\Lambda}$ (cm)	σ_Λ (cm)
BBQ	1	254	17
	2	350	27
Yellow 323	1	44	3
	2	52	8

* Product of Valvo, Hamburg, West Germany.
** Product of Scott, Mainz, West Germany.
§ Product of Dow Corning Corporation, Midland, Michigan, USA.
§§ Product of Röhm GmbH, Darmstadt, West Germany.

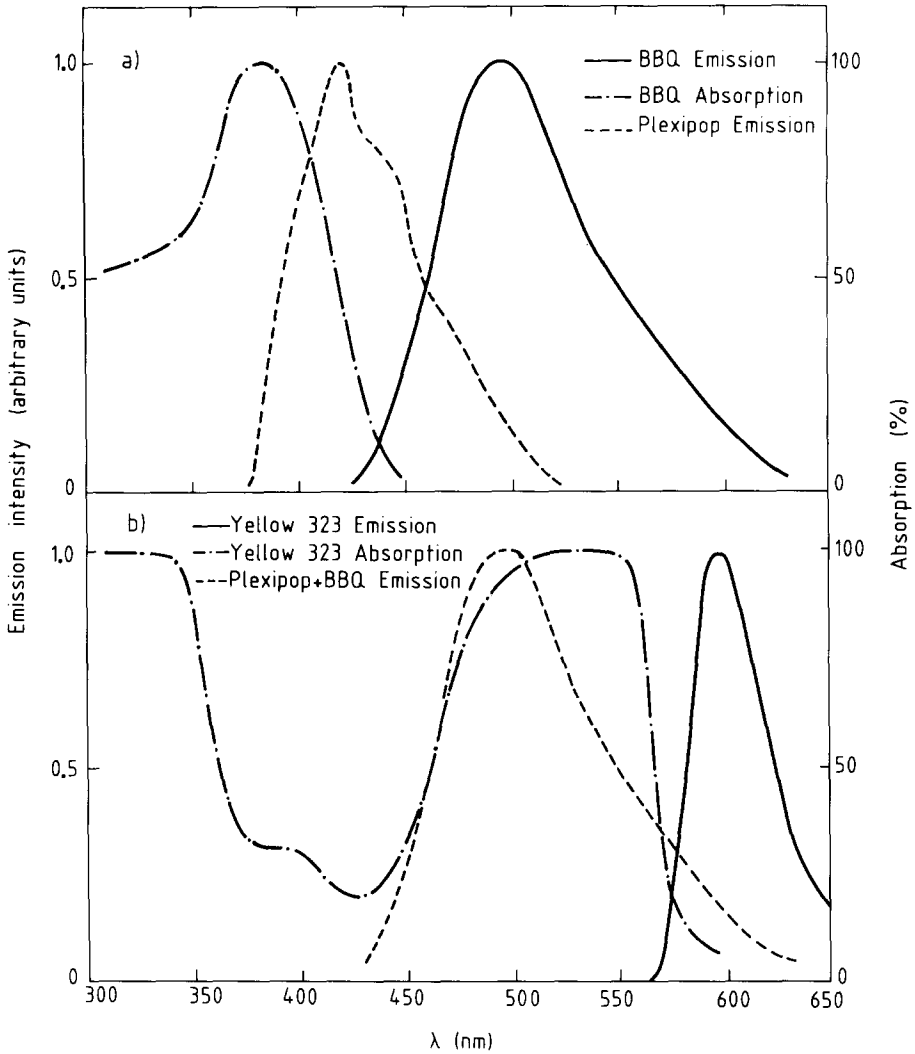

Fig. 4. The emission spectra of the scintillator materials and the emission and absorption spectra for the wavelength shifter rods are shown (a) for the hadron section and (b) for the photon section of the calorimeter. All emission spectra were supplied by Röhm GmbH in Darmstadt, W. Germany.

packed into plastic trays as shown in fig. 6. Each tray is subdivided into ten optically isolated compartments to prevent cross talk from one cell to another. The plastic walls of the tray are 1 mm thick. The 2.5 mm thick bottom and cover plate of the tray were coated with reflective aluminized mylar. The edges of the scintillators were cut, left unpolished, and were painted with white TiO_2 paint to reflect some of the escaping light back into the scintillator. Our measurements have shown that somewhat better light yields can be obtained with painted scintillator edges than with polished edges in connection with aluminum reflectors. The surface of the holes in the scintillators was left unpolished in order to obtain diffuse light scattering from the scintillator into the rods. In this way time consuming and expensive polishing of the scintillator edges and holes was avoided. The trays with the scintillator were then one by one inserted and fixed between the iron disks.

The scintillators in the photon calorimeter were treated in the same way as described above. They were inserted in between the lead converter plates as shown in fig. 7. The ten cells per sector are separated by I-shaped aluminum spacers (1.2 mm thickness). These spacers prevented cross talk from one cell to the neighbouring cell and also kept the lead sheets from touching the scintillator surface. The mechanical strength of each photon calorimeter sector was provided by a 2 cm thick aluminum plate in front and a 3 cm thick aluminum plate in back. The sectors were made light tight by 1 mm thick steel sheets on the sides. Each

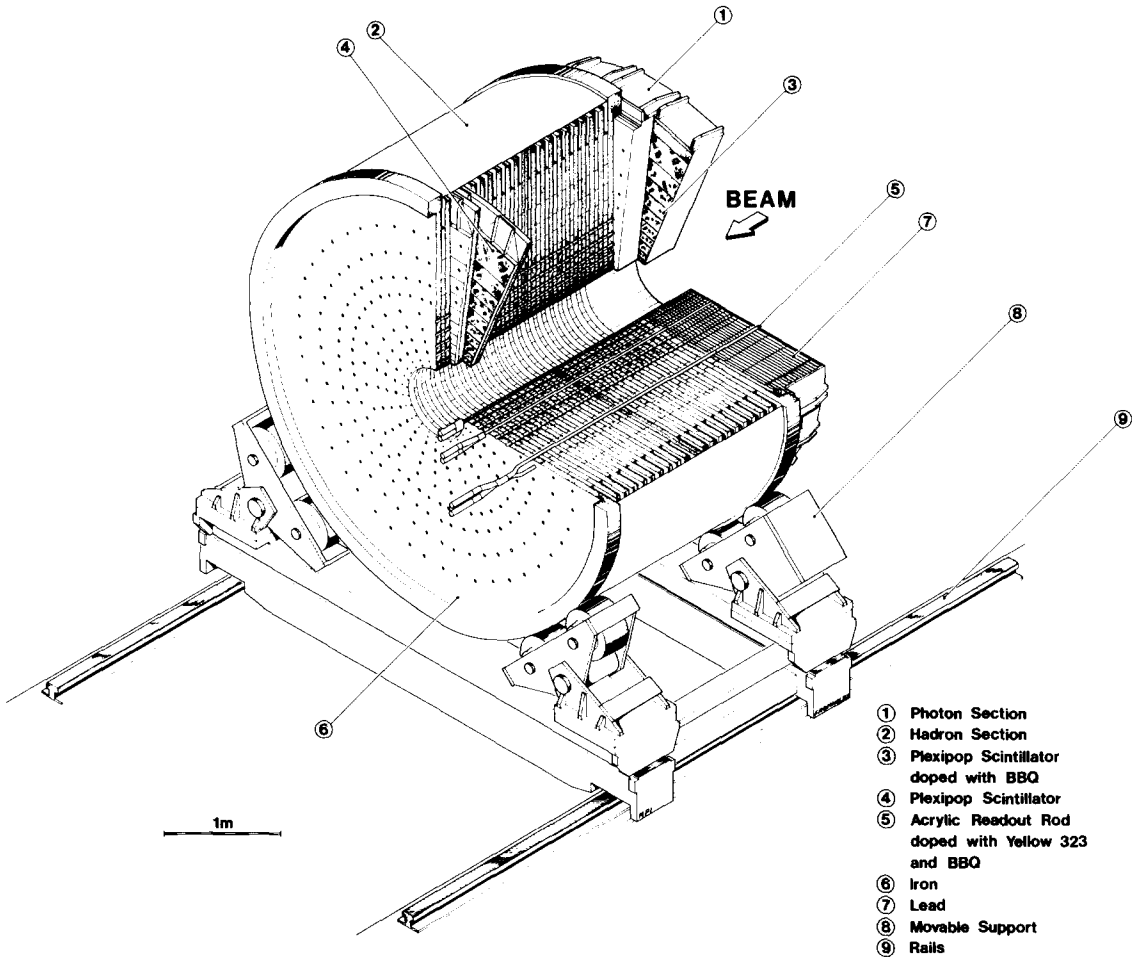

Fig. 5. Perspective view of the ring calormimeter.

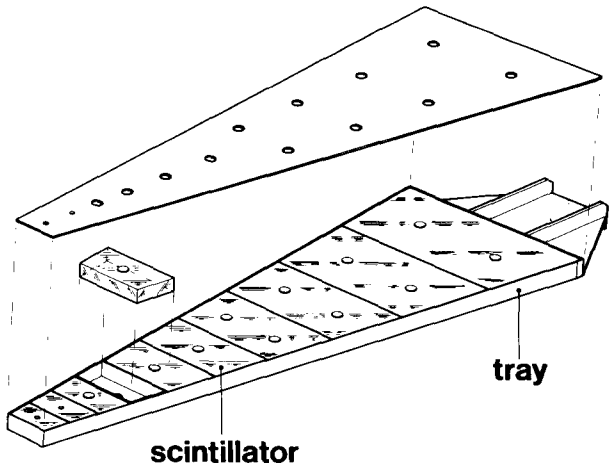

Fig. 6. One of the plastic trays with scintillators inside.

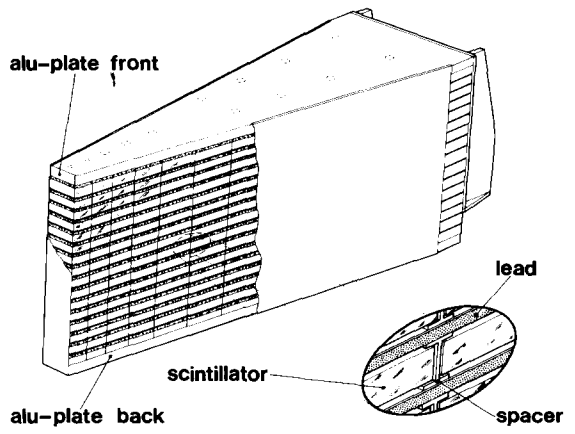

Fig. 7. Perspective view of one ot the photon calorimeter sectors.

of the 24 sectors was mounted tight onto the front disk of the hadron calorimeter. The gap between neighbouring sectors was a few mm.

After the mounting of the photon sectors and the scintillator trays of the hadron calorimeter the optical readout rods were inserted from the back side of the calorimeter.

2.3. Performance

2.3.1. Calibration

The calorimeters were set up in the H_2 beam-line of the SPS North Area. The ring calorimeter was calibrated with incident muons, electrons and negative pions at 60 GeV. The electrons and pions in the beam were selected by 2 CEDAR Cherenkov counters. The muons were identified by a small counter downstream of the calorimeters. The movable support structure described above allowed every cell of the calorimeter to be moved into the incident beam line.

For each cell the photomultiplier gains were adjusted such that 60 GeV electron showers in the photon section gave the same peak pulse height as 60 GeV hadron showers in the hadron section of the calorimeter. The lateral shower spread was taken into account by adding the energy deposited in the surrounding cells. This was particularly important for hadron showers and for the calibration of the small size cells.

For hadrons which started showering in the photon section the energy measured by this section was multiplied by a weighting factor before adding it to the energy measured in the hadron section. The best hadron energy resolution was obtained with a weighting factor of 1.6.

The photomultiplier gains were monitored by using light-emitting diodes and optical fibers as described in ref. 7.

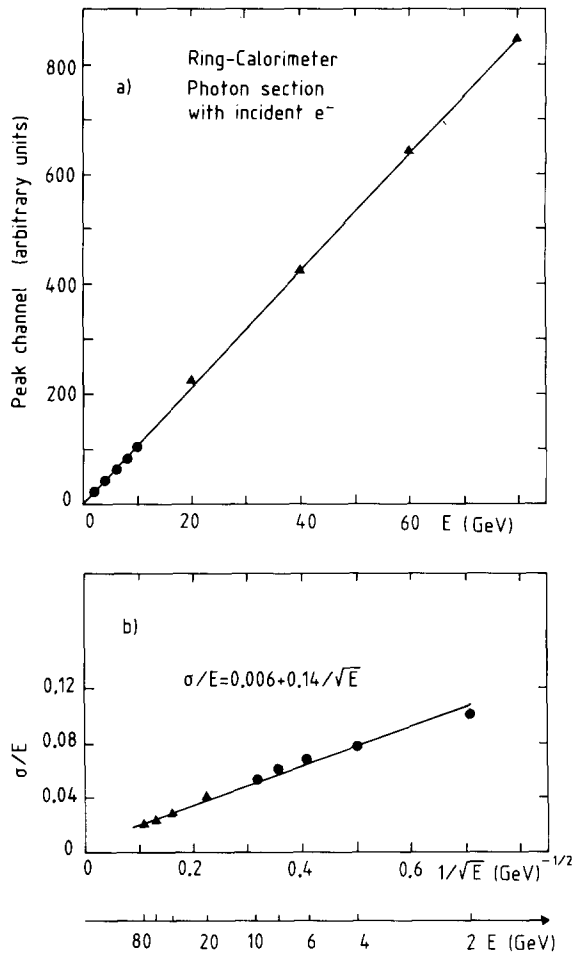

Fig. 8. (a) The peak pulse height as a function of the incident electron energy and (b) the energy resolutions σ/E are shown for the photon section of the calorimeter. The triangles and the points are the results obtained with the ring and the test calorimeter respectively.

2.3.2. Energy resolution and linearity of response

The resolution and the linearity of energy response of the ring calorimeter were measured in the energy range 20–80 GeV. The lowest available incident beam energy was limited to 20 GeV in this beam line for operational reasons. In order to obtain information on the calorimeter performance at lower energies we built a small size test calorimeter module resembling one of the large size cells in the ring calorimeter and moved it into a low energy beam line (2–10 GeV) in the South Hall of the PS.

The measured peak pulse heights as a function of energy are shown in figs. 8a and 9a for the photon and the hadron section respectively. For these measurements the incident beam was impinging near the center of the cell #9. As can be seen the calorimeter shows a linear energy response up to the highest measured beam energy of 80 GeV. An independent test of the linear energy response of the calorimeter to secondary hadrons produced in a hydrogen target of the NA5 experiment is shown in fig. 10. The momenta of the secondary hadrons (they were assumed to be pions) measured with the NA5 streamer chamber vertex spectrometer agree with th energy measured in the calorimeter.

In figs. 8b and 9b the energy resolutions, σ/E, obtained for incident e^- and π^- of various energies are shown as a function of $1/\sqrt{E}$, with E in GeV. A linear fit through the data points gives an energy resolution of $\sigma/E = 0.006 + 0.14/\sqrt{E}$ for incident electrons and $\sigma/E = 0.03 + 0.64/\sqrt{E}$ for incident pions. The data have not been corrected for possible energy losses of incident electrons radiating in the material upstream of the calorimeter.

In the case of the photon section of the calorimeter

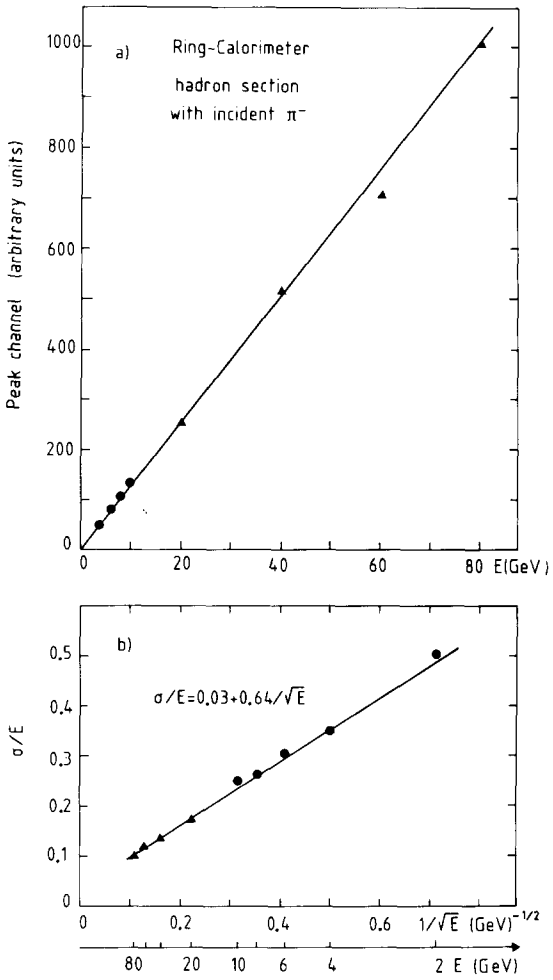

Fig. 9. (a) The peak pulse height as a function of the incident pion energy and (b) the energy resolutions σ/E are shown adding the information of the photon and hadron section as described in the text. The triangles and the points are the results obtained with the ring and the test calorimeter respectively.

the sampling fluctuation part of the resolution can be estimated from the empirical formula [8,9]:

$$\left(\frac{\sigma}{E}\right)_s \sim \sqrt{\frac{1}{Ne \cdot E}},$$

where E is the incident electron energy in GeV and Ne is the number of equivalent minimum ionizing particles observed per GeV of electron energy deposited in the calorimeter. Ne was determined by comparing measurements with incident muons and electrons and found to be 44. We thus compute $(\sigma/E)_s \sim 13\%/\sqrt{E}$, showing that the energy resolution of the photon section of the calorimeter is dominated by sampling fluctuations.

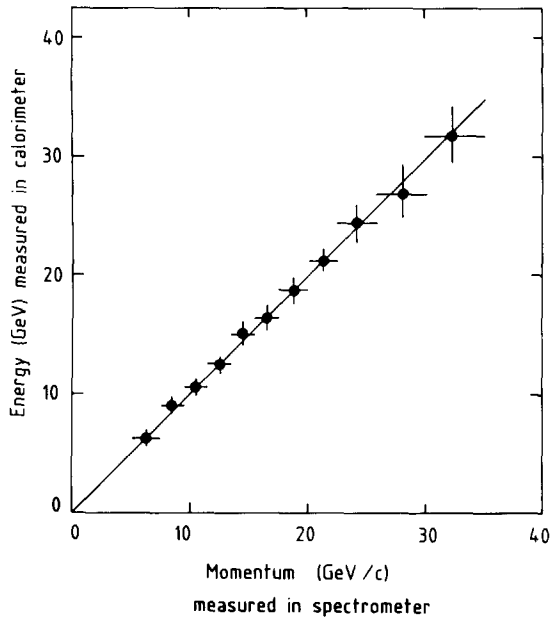

Fig. 10. Energy deposited in the calorimeter vs the momentum measured in the spectrometer for charged particles assuming they are pions. The error bars on the ordinate represent the precision of determining the peak pulse height. The error bars on the abscissa represent the bin size.

2.3.3. Cross talk between the photon and the hadron section

Even with the use of an OG 570 filter between the Yellow and the BBQ part of the rods a small amount of cross talk between the photon and the hadron section of the calorimeter still remained. This was measured by two independent methods:

In one case the part of the rods in the hadron (photon) section was wrapped in black paper and the pulse height due to cross talk was measured in that section with incident electrons (hadrons) at various energies.

In the other case the cross talk was evaluated from the pulse height correlations observed in the photon (hadron) section for hadron (photon) showers which were fully contained in the hadron (photon) section of the calorimeter.

The amount of cross talk was measured to be different for different cells. Most likely this is a result of how well the cross sectional area of the different rods were covered by the filters. On average we obtained a cross talk of 6.2% from electron showers into the hadron section of the calorimeter. For comparison the electromagnetic shower containment in the photon section, which represents a total of 19.5 radiation lengths, was measured to be 96% with incident electrons of 80 GeV.

The measured cross talk from the hadron into the

photon section was on average 3.5%. This small amount of cross talk did not turn out to be a problem for discriminating between electromagnetic and hadronic showers.

2.3.4. Uniformity

The uniformity of response of the calorimeter was studied with electrons and pions of 60 GeV by performing a scan through cell #5 and cell #6 as shown in fig. 11. The incident beam size was defined by a 1 cm diameter counter. In the course of this scan the incident beam axis was parallel to the readout rods. Figs. 11a, b, c shows for incident electrons and pions the ratio of the peaks of the pulse height distributions measured at the indicated points along the x-, u- and y-axis to that obtained at the calibration point. The results show that the peak pulse height increases when the incident beam hits near the readout rods. The effect is more pronounced with incident electrons than with hadrons. Electron showers are much narrower than hadron showers, therefore they are more affected by the transition regions, i.e. the edges of a cell and the vicinity of the readout rods. The observed non-uniformity is mainly due to three effects:

(1) Particles will escape detection if they hit the region between individual cells and sectors.

(2) Particles which cross the readout rods induce Cherenkov light in the rods. This effect has been estimated from a measurement in which the readout rods have been covered with black paper in order to completely shield them against the light coming from the scintillators. With the covered rods, a pulse height distribution due to induced Cherenkov light was measured for incident hadrons of 10 GeV impinging at a distance of 3 cm from the readout rod axis. Using Monte Carlo methods this distribution was folded with a pulse height

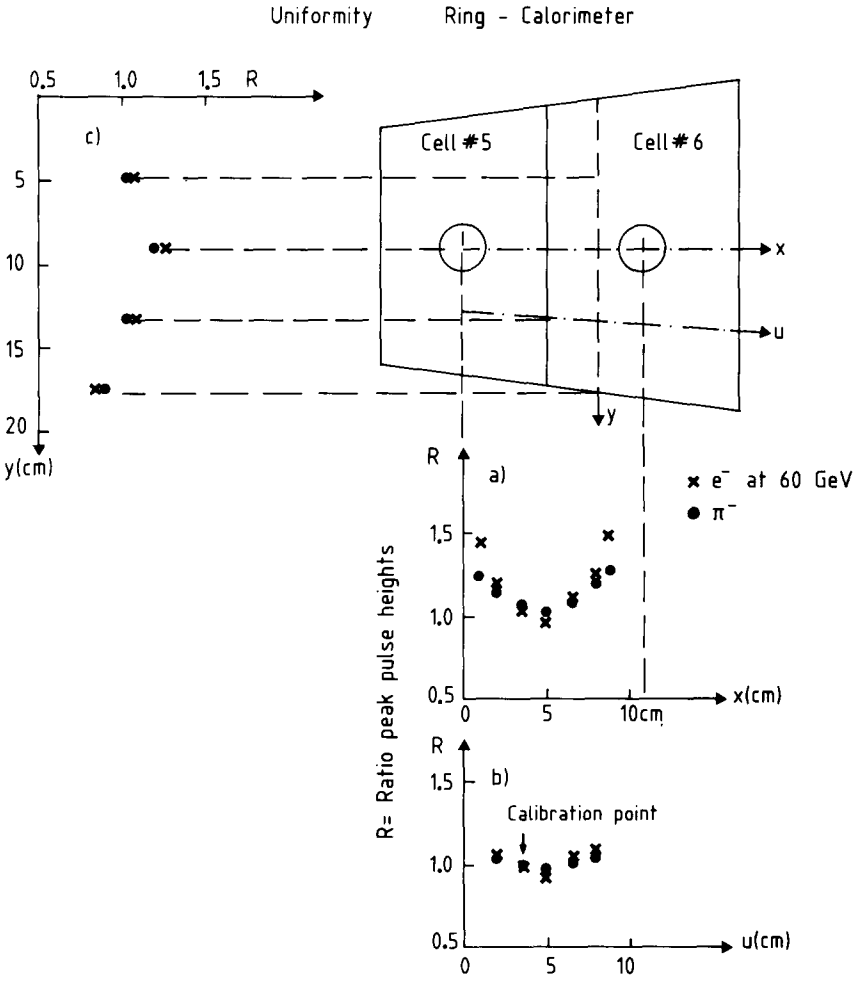

Fig. 11. The ratio of the peak of the pulse height distributions measured along (a) the x-, (b) the u- and (c) the y-axis respectively to that measured at the calibration point. The scan was performed with the incident beam travelling parallel to the readout rods.

distribution (peak channel 106) obtained with uncovered readout rods and with an incident beam impinging far away from the readout rods. The resulting distribution (peak channel 120) was then compared to the pulse height distribution (peak channel 133) obtained with uncovered rods for the original beam position of 3 cm distance from the readout rod axis. This measurement shows that out of the total observed non-uniformity of 25% only approximately half can be attributed to induced Cherenkov light.

(3) For particles which traverse the scintillator near the readout rods additional ultra-violet (UV) scintillator light (with wavelength shorter than the POPOP emission) can reach the readout rods. This additional UV light will normally be absorbed in the scintillator material for particles traversing at a larger distance from the rods.

Inhomogeneities of the calorimeter response due to Cherenkov light and additional UV light have also been studied in refs. 10 and 11. The effect of Cherenkov light produced in the readout rods can in the future be reduced by using w.s. rods with and UV absorbing chemical [10], which absorbs part of the Cherenkov light before it is converted by the BBQ or the Yellow 323 w.s., and by using rods with smaller cross-sections [12]. By inserting UV absorbing filters between the scintillators and the w.s. rods, the non-uniformity due to additional UV scintillator light can be reduced.

The results of the uniformity scan shown in fig. 11 were obtained with incident particles travelling parallel to the readout rods, which run parallel to the axis of the calorimeter (projective geometry). In the NA5 experiment however all secondary particles originating from an upstream target traverse the calorimeter cells at an angle (non-projective geometry). It was not possible to study the effects of a non projective geometry with the ring calorimeter in situ. We therefore used the test calorimeter in a 20 GeV test beam of the SPS West Area. We performed measurements with the incident particle beam impinging at various distances from the readout rods and at typical angles of incidence (3°-9.4°). It was found that the uniformity of response was considerably improved when particles crossed the calorimeter cells at an angle. The measured non-uniformity of response from a scan across a calorimeter cell was $\leqslant 15\%$ ($\leqslant 5\%$) for an angle of incidence of 3°(9.5°) when the incident beam crossed the readout rods and $\leqslant 4\%$ ($\leqslant 4\%$) when it did not.

3. Downstream calorimeter

The downstream calorimeter was positioned immediately behind the ring calorimeter. Its purpose was to measure the energy flow of particles passing through the central hole of the ring calorimeter. Its mechanical construction is shown in fig. 12. The downstream calorimeter was subdivided into a photon section and a

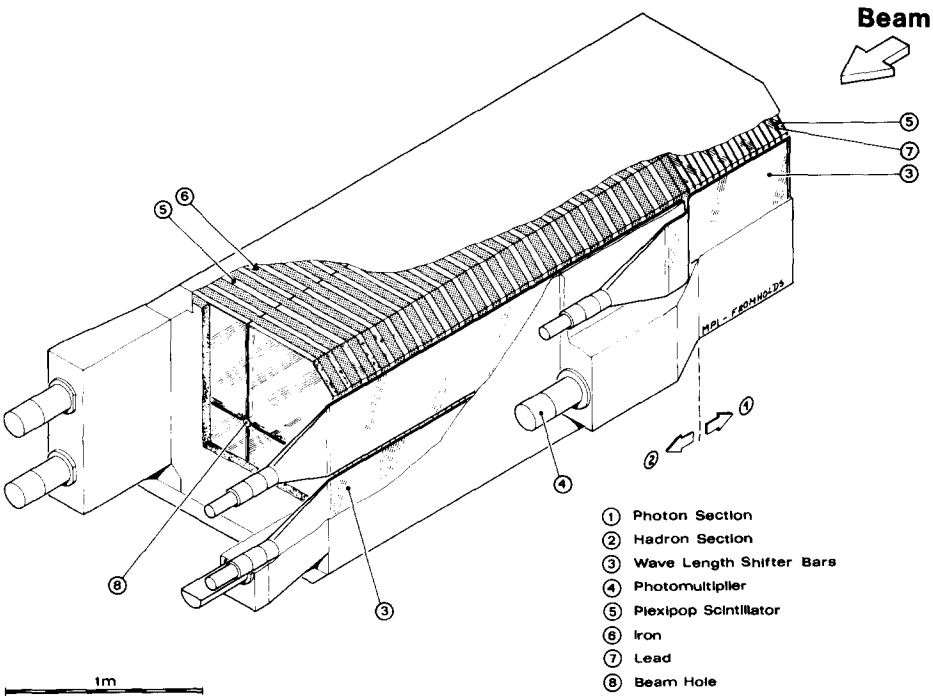

Fig. 12. Perspective view of the downstream calorimeter.

hadron section. Each section was segmented into 4 cells. A small hole of 2.5 cm diameter in the center allowed the non-interacting incident beam to pass through.

3.1. Mechanical construction

The sensitive area of the downstream calorimeter has an octogonal shape and covers approximately 1×1 m^2. The size of the downstream calorimeter is well matched to measure the energy flow of particles passing through the central hole of the ring calorimeter. It also efficiently detects the leaking particles from showers produced in the ring calorimeter near its central hole.

The photon section consists of 16 layers of 5.5 mm thick lead sandwiched with 2.5 cm Plexipop scintillator. The lead was glued between two aluminum plates, each 1 mm thick, to provide mechanical strength. The following hadron section contained 25 layers of 5 cm thick iron sandwiched with 2.5 cm thick Plexipop scintillator. The hadron section of the calorimeter was lengthened by 5 layers as compared to the hadron section of the ring calorimeter in order to obtain better longitudinal shower containment for more energetic particles at smaller scattering angles.

The scintillator light in the photon and the hadron calorimeter cells was read out by BBQ doped Plexibars as indicated in fig. 12. The bars were 1 cm thick and 37 cm wide. The w.s. bars were glued to a triangular shaped Plexi light guide (Plexi 2000) * which absorbed light with wavelength less than 450 nm. This highly absorptive Plexi material was selected to reduce the Cherenkov light in the light guides. The scintillator and w.s. materials which were used are listed in table 3. The eight light guides were glued to XP 2030 PMs **.

The downstream calorimeter was mounted on a movable support structure, which served similar functions as in the case of the ring calorimeter.

3.2. Performance

3.2.1. Energy resolution and linearity of response

The calorimeter was exposed to incident electrons in the energy range of 15 GeV to 100 GeV and to pions in the energy range of 15 GeV to 340 GeV. The measured energy resolutions and the linearity of response are shown in figs. 13 and 14 for incident electrons and pions respectively. A linear fit through the data points in fig. 13b and 14b gives an energy resolution of $\sigma/E = 0.17/\sqrt{E}$ for incident electrons and $\sigma/E = 0.03 + 0.74/\sqrt{E}$ for incident pions. The data have not been corrected for possible energy losses of incident electrons radiating in material upstream of the calorimeter.

* Manufactured by Röhm GmbH, Darmstadt, West Germany.
** Product of Valvo, Hamburg, West Germany.

Table 3
The scintillator and wavelength shifter bars used in the photon and hadron section of the downstream calorimeter.

	Material	Doped with	Thickness (cm)
Scintillator	Plexipop [a]	3% Naphtalene 1% Butyl PBD 0.03% POPOP	2.5
w.s. bar	Plexi 201 [a]	150 mg/l BBQ	1.0

[a] Manufactured by Röhm GmbH, Darmstadt, West Germany.

3.2.2. Uniformity

We studied the uniformity of response of the calorimeter with 60 GeV electrons and pions by performing a scan through one of the calorimeter cells as indicated in fig. 15. In order to account for shower leakage into the neighbouring cells the pulse heights of

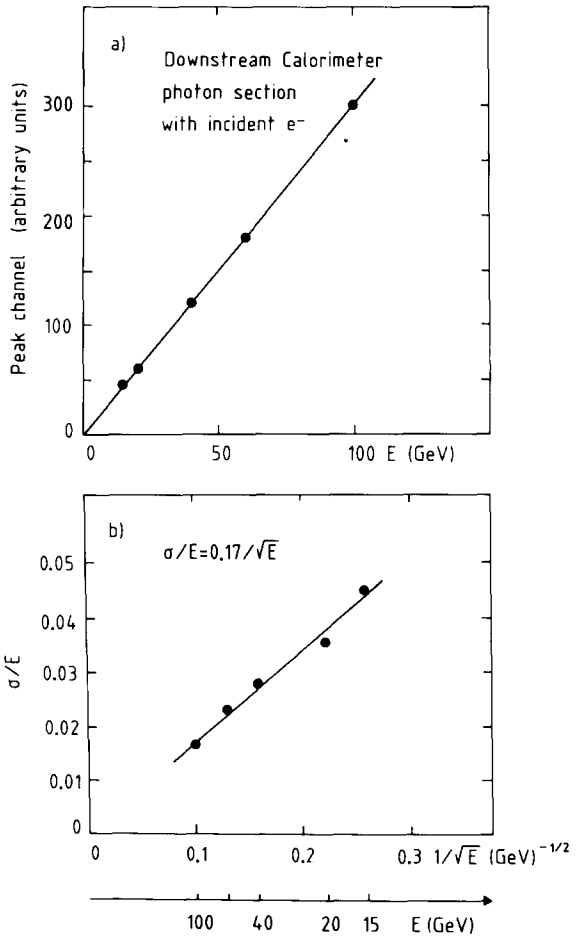

Fig. 13. (a) The peak pulse height as a function of the incident electron energy and (b) the energy resolutions σ/E are shown for the photon section of the calorimeter.

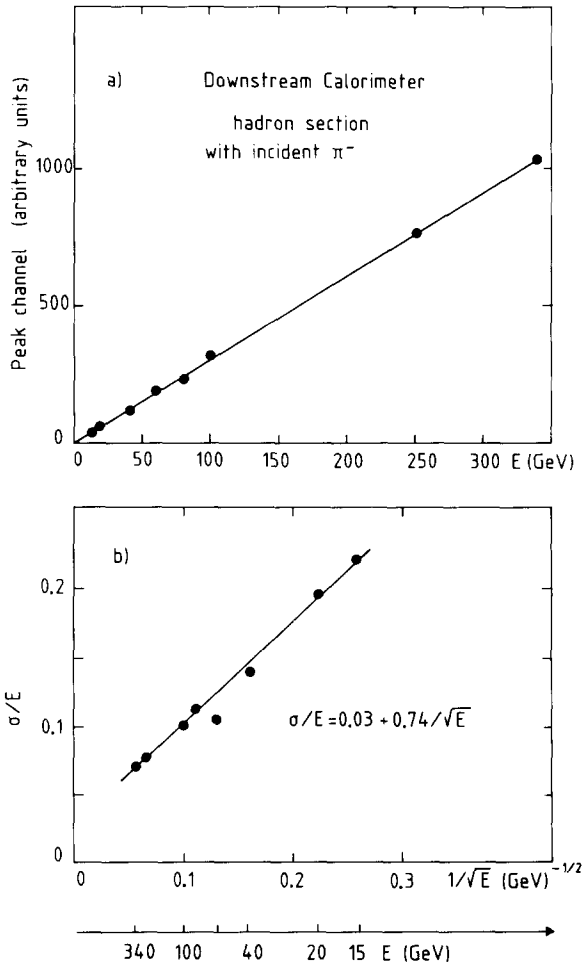

Fig. 14. (a) The peak pulse height as a fuanction of the incident pion energy and (b) the energy resolutions σ/E are shown adding the information of the photon and hadron section as described in the text.

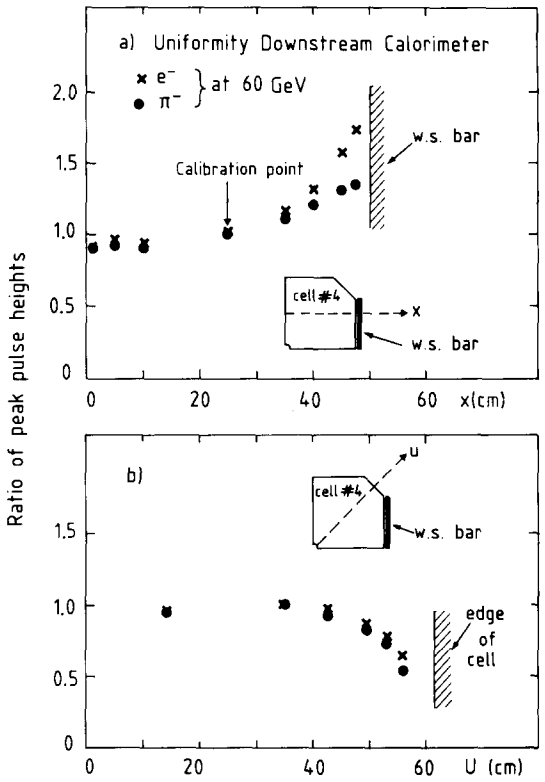

Fig. 15. The ratio of the peaks of the pulse height distributions measured along (a) the x- and (b) the u-axis respectively to that measured at the calibration point. The scan was performed with the incident beam travelling parallel to the calorimeter axis.

those were added in the total sum. As shown in fig. 15 the calorimeter response is non-uniform when the incident particles impinge near the wave shifter bars. As observed previously this effect is more pronounced with incident electrons than with incident hadrons. In the case of incident hadrons the transverse shower leakage out of the calorimeter cell is somewhat compensated by the effects leading to inhomogeneities in response as discussed in sect. 2.3 of this paper.

4. Conclusions

The optical readout system described here allowed a compact and economical construction of a segmented photon–hadron calorimeter. It has the advantage that the light collection of a cell in the photon section and of a cell in the hadron section can be incorporated into one common readout rod. By locating all photo-multiplier tubes behind the calorimeter an unsuitable environment for the tubes such as high magnetic field or a region of high particle flux was avoided.

The most serious limitation of the system is the non-uniformity of response in the vicinity of the light collecting holes. It has been shown that this problem is markedly reduced, when particles cross the calorimeter cells at an angle (non-projective geometry). The uniformity can further be improved in the future by inserting ultraviolet absorbing filters between the scintillators and the readout rods and by reducing the cross sectional area of the readout rods, as proposed in ref. 12.

We thank Dr. Fischer and Mr. Widhalm of the Röhm GmbH, Darmstadt, West Germany for their helpful cooperation. We are indebted to Messrs. H. Münch, H. Stieg, E. Giesche, W. Tribanek and P. Sawallisch of the Max Planck Institut für Physik and Astrophysik in München and A. Degano of the Bari University and INFN section, Italy, and their colleagues in

both institutes for building the apparatus. It is a pleasure to acknowledge the contributions of A. Sacchetti to the electronic part of the calorimeter. Finally we would like to thank the CERN SPS and PS coordinators and the operating crews for their excellent support.

References

[1] C. de Marzo et al., Phys. Lett. 112B (1982) 173.
[2] C. de Marzo et al., Nucl. Phys. B211 (1983) 375.
[3] V. Eckardt et al., Nucl. Instr. and Meth. 155 (1978) 389.
[4] W.A. Schurcliff, J. Opt. Soc. Am. 41 (1951) 209.
[5] R.C. Garwin, Rev. Sci. Instr. 31 (1960) 1010.
[6] G. Keil, Nucl. Instr. and Meth. 83 (1970) 145;
G. Keil, Nucl. Instr. and Meth. 87 (1970) 111.
[7] M. de Palma et al., Nucl. Instr. and Meth. 190 (1981) 41.
[8] U. Amaldi, CERN-EP/80-212.
[9] C.W. Fabjan and T. Ludlam, Ann. Rev. Nucl. Part. Sci. 32 (1982) 335.
[10] O. Botner et al., Nucl. Instr. and Meth. 179 (1981) 45.
[11] M.A. Schneegans et al., Nucl. Instr. and Meth. 193 (1982) 445.
[12] J. Fent et al., Nucl. Instr. and Meth. 211 (1983) 315.